Supplementary Material:
Patchy particles by self-assembly of star copolymers on a spherical substrate: Thomson solutions in a geometric problem with a color constraint

Tobias M. Hain,[a,c], Gerd E. Schröder-Turk*[a,b,c] and Jacob J. K. Kirkensgaard*[b]

[a] *College of Science, Health, Engineering and Education, Mathematics and Statistics, Murdoch University, 90 South Street, 6150 Murdoch, Western Australia, Australia*
[b] *Department of Food Science, University of Copenhagen, Rolighedsvej 26, 1958 Frederiksberg, Copenhagen, Denmark*
[c] *Physical Chemistry, Department of Chemistry, Lund University, P.O. Box 124, 221 00 Lund, Sweden*
* G.Schroeder-Turk@murdoch.edu.au, jjkk@food.ku.dk

1 Frequency of Thomson solutions in simulation runs

R	N	frames found	Proportion [%]
4	2	300	100
5	2	210	70
5	3	90	30
6	3	95	31.7
6	4	205	68.3
7	4	180	60
7	5	120	40
8	5	15	5
8	6	285	95
9	6	165	55
9	7	120	40
9	8	15	5
10	8	67	22.3
10	9	233	77.7

R	N	frames found	Proportion [%]
4	2	900	100
5	2	31	3.4
5	3	428	47.6
5	4	441	49
6	3	1	0.1
6	4	614	68.2
6	5	105	11.7
6	6	180	20
7	5	92	10.2
7	6	794	88.2
7	7	14	1.6
8	6	128	14.2
8	7	425	47.2
8	8	282	31.3
8	9	50	5.5
8	NT	9	1
8	INV	6	0,7
9	8	129	14.3
9	9	626	69.5
9	10	27	3
9	NT	104	11.5
9	INV	14	1.5
10	10	93	10.3
10	11	370	41.1
10	12	29	3.2
10	NT	398	44.2
10	INV	10	1.1

Table 1 Frequencies and numbers of equilibrium solutions for ABB (left table) and ABC (right table) systems The table lists the values fig. (6) in the main article is generated from. Shown are the absolute numbers and the frequencies of which equilibrium solutions are found in multiple runs of the simulations.

2 Characterization of Non-Thomson solutions

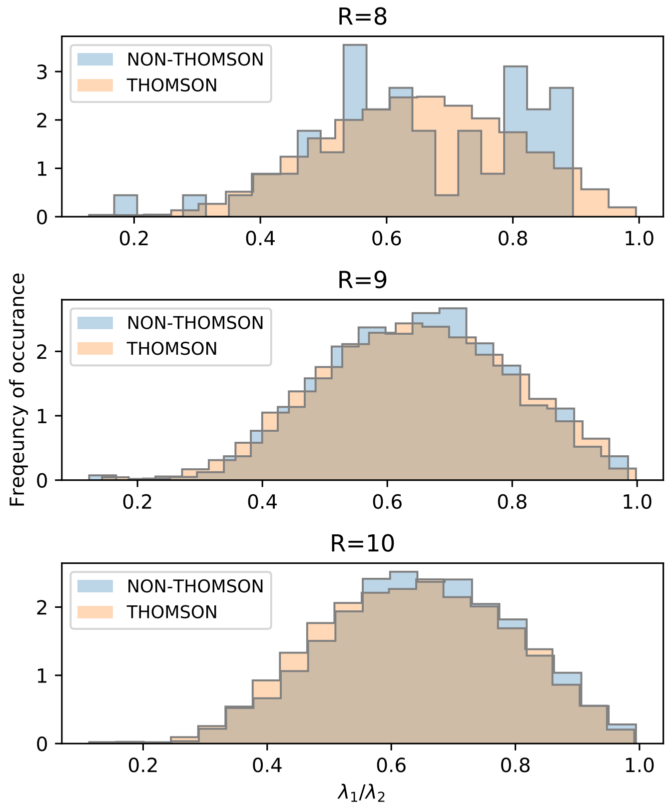

Figure 1 Shape metrics describing the anisotropy of the patches Shown is the distribution of the dimensionless ratio of the two smaller eigenvalues $\frac{\lambda_1}{\lambda_2}$ of the tensor of inertia $I_{ij} = \sum_l^{N_k} \left(||\mathbf{x}_l||^2 \delta_{ij} - x_i x_j \right)$ computed for each patch k. Here $\mathbf{x}_l$ is the position of particle l in the cluster k and N_k is the number of particles associated with the cluster. The tensor of inertia can be represented by a 3×3 matrix and provides information about the mass distribution of a body in 3D space. Its eigenvalues equal to the moments of inerta around its principal axes. In case of sphere caps the largest eigenvalue corrseponds to the principal axis in radial direction, where as the two smaller eigenvalues correspond to the two tangential directions. For a spherical cap these are degenerate and their ratio $\frac{\lambda_1}{\lambda_2}$ equals to one. If the cap is distorted to a ellipsoidal shape one of the eigenvalues will increase, resulting in a decreasing ratio $\frac{\lambda_1}{\lambda_2}$. Hence, the smaller the ratio of the smaller eigenvalues, the more distorted the cap is from a spherical shape. The slight differences which can be seen in the distributions of eigenvalue fractions of Thomson and non-Thomson solutions in the figure of our preliminary analysis are too small to be of statistical significance. Therefore we can find no correllation between the patch shape and the type of the tiling.

2.1 List of Non-Thomson solutions found in our analysis

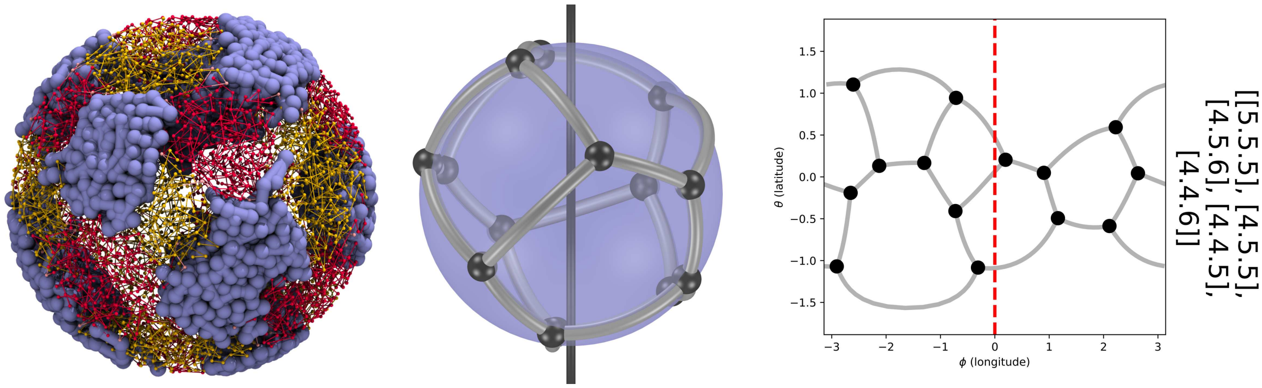

Figure 2 Non-Thomson solution for $N = 9$ patches with 4 squares, 4 pentagons and 1 hexagon.

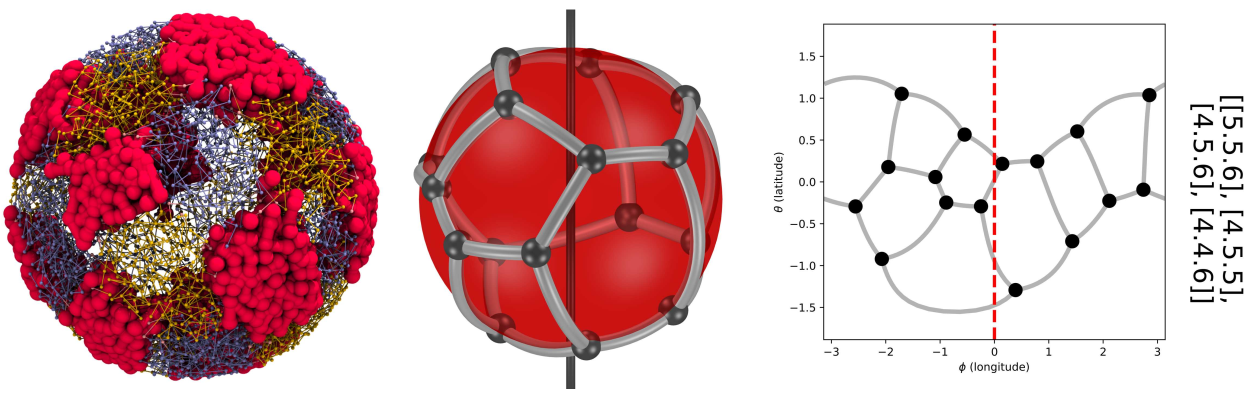

Figure 3 Non-Thomson solution for $N = 10$ patches with 4 squares, 4 pentagons and 2 hexagon.

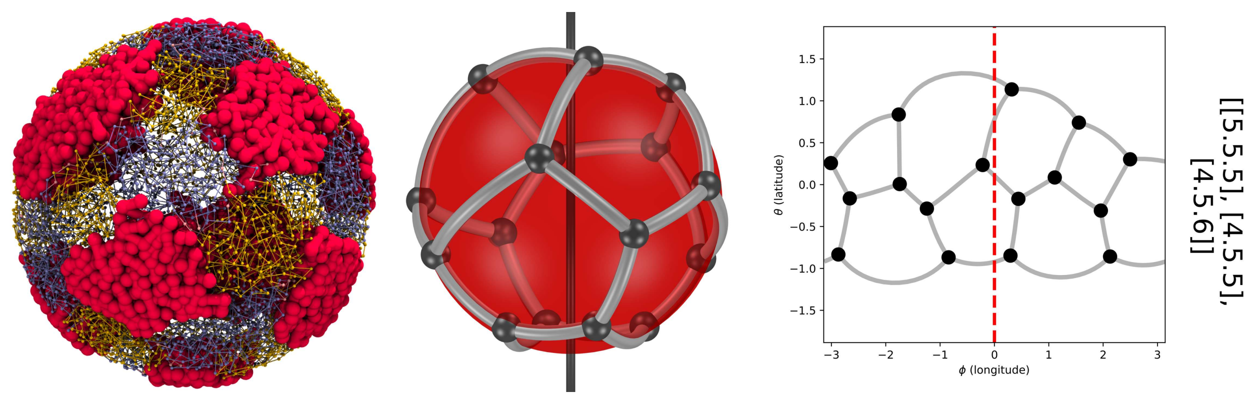

Figure 4 Non-Thomson solution for $N = 10$ patches with 3 squares, 6 pentagons and 1 hexagon.

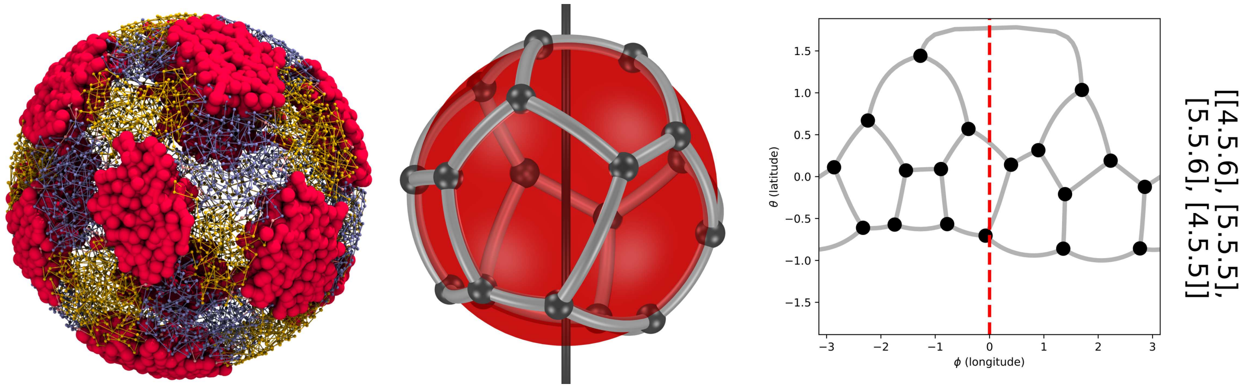

Figure 5 Non-Thomson solution for $N = 11$ patches with 3 squares, 6 pentagons and 2 hexagon.

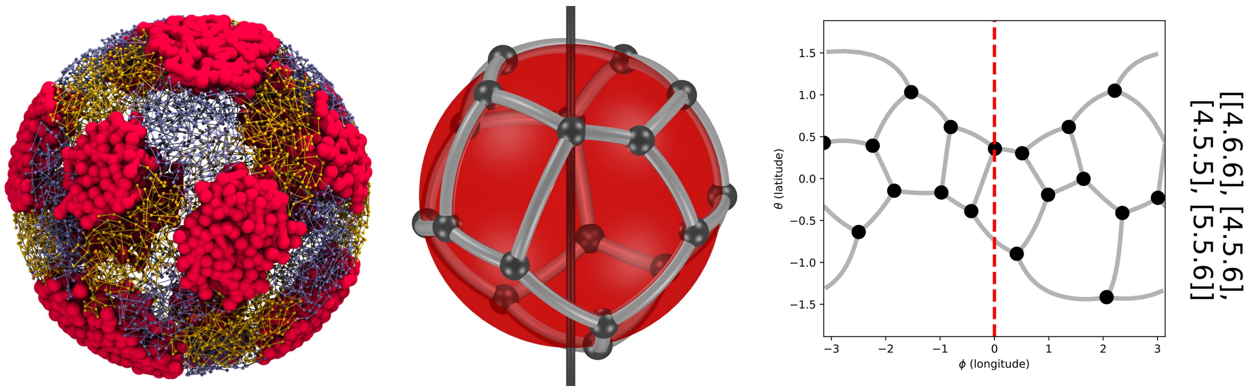

Figure 6 Non-Thomson solution for $N = 11$ patches with 4 squares, 4 pentagons and 3 hexagon.

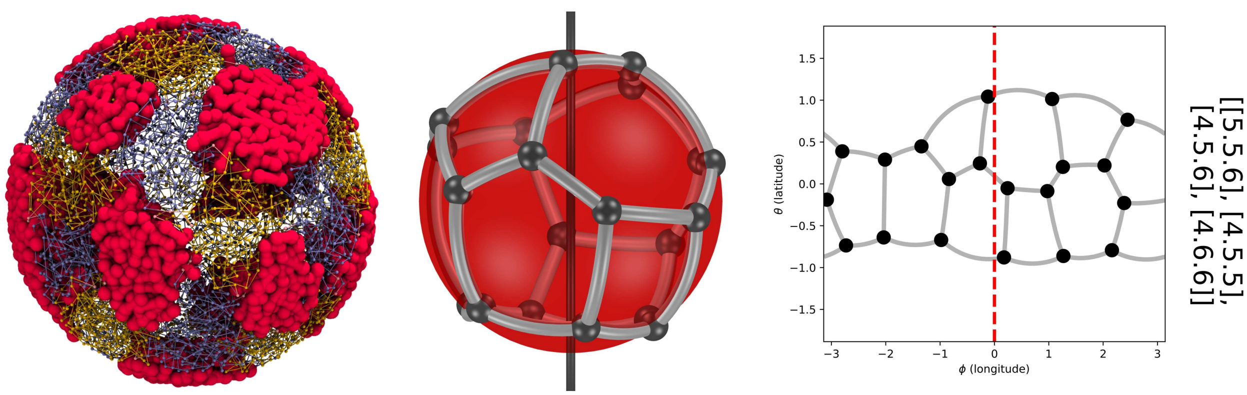

Figure 7 Non-Thomson solution for $N = 12$ patches with 4 squares, 4 pentagons and 4 hexagon.

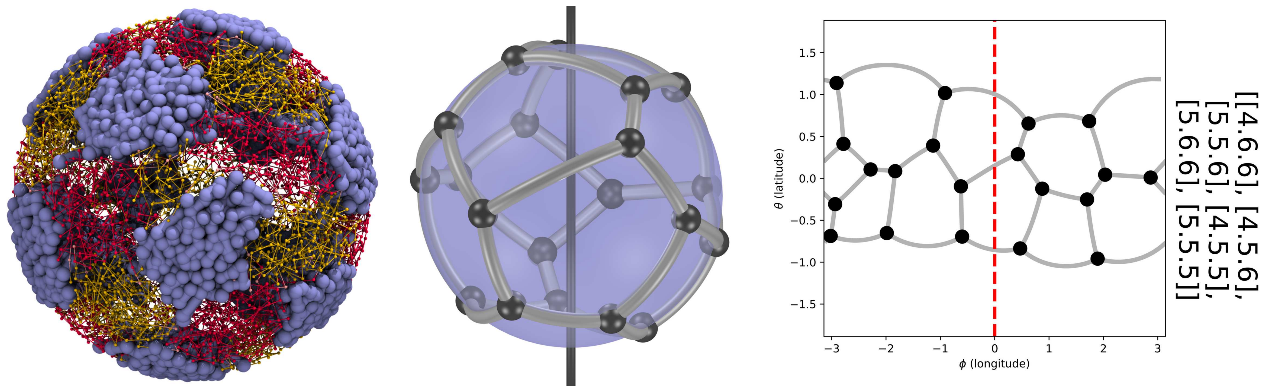

Figure 8 Non-Thomson solution for $N = 12$ patches with 3 squares, 6 pentagons and 3 hexagon.

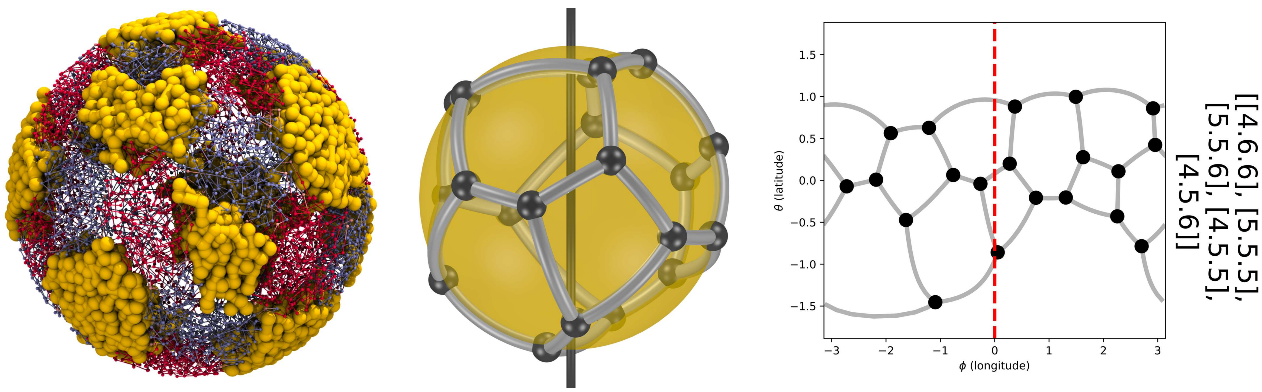

Figure 9 Non-Thomson solution for $N = 12$ patches with 2 squares, 8 pentagons and 2 hexagons.

3 Radius of gyration of *ABB* and *ABC* star copolymers

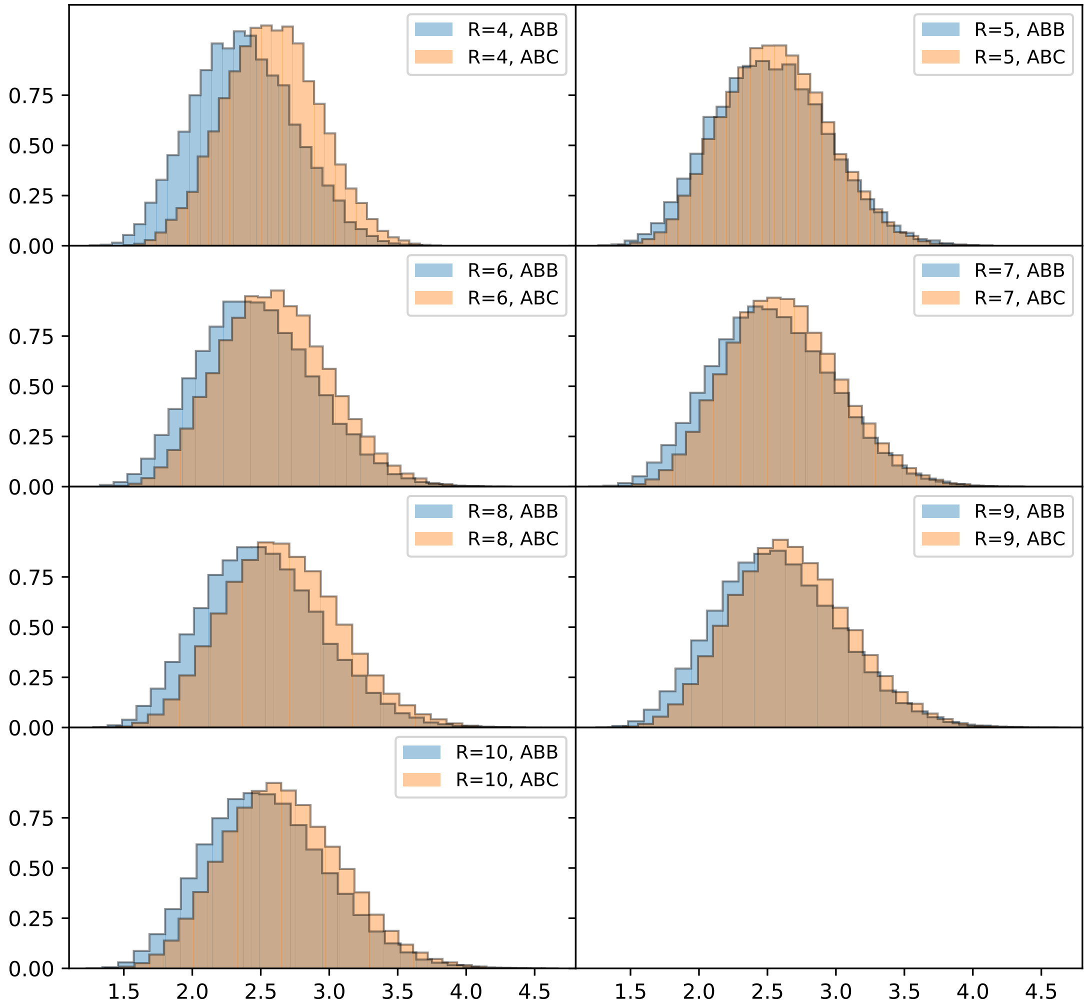

Figure 10 Distribution of radii of gyration of *ABC* star copolymers confined to a spherical shell The figure shows the radius of gyration $R_G = \sqrt{\frac{1}{N}\sum_i^N \mathbf{r}_i^2}$, where the sum runs over all beads in the polymer and $\mathbf{r}_i$ is the vector from the i-th bead to the center of mass of the polymer[1], for all polymers in the analyzed frames in terms of the length unit $\mathscr{D}$. All data is shown for a shell width of $dR = 2\mathscr{D}$. The figure shows that polymers in the *ABB* system are slightly more compact than in an *ABC* system.

References

[1] M. Fixman, *The Journal of Chemical Physics*, 1962, **36**, 306–310.